

Article

Impacts of Array Orientation and Tilt Angles for Photovoltaic Self-Sufficiency and Self-Consumption Indices in Olive Mills in Spain

Gabino Jiménez-Castillo ^{1,*}, Francisco José Muñoz-Rodríguez ^{1,2},
Antonio Javier Martínez-Calahorra ¹, Giuseppe Marco Tina ³ and Catalina Rus-Casas ^{1,2}

¹ Department of Electronic and Automatic Engineering, Universidad de Jaen, 23071 Jaen, Spain;

fjmunoz@ujaen.es (F.J.M.-R.); antoniojavier.martinez@ujaen.es (A.J.M.-C.); crus@ujaen.es (C.R.-C.)

² Centre for Advanced Studies in Energy and Environment CEAEMA, Universidad de Jaen, 23071 Jaen, Spain

³ Department of Electrical, Electronics and Computer Engineering, University of Catania, 95125 Catania, Italy; giuseppe.tina@unict.it

* Correspondence: gjimenez@ujaen.es

Received: 31 December 2019; Accepted: 14 February 2020; Published: 18 February 2020



Abstract: Olive mills are extensive in the Mediterranean Basin, and Spain constitutes approximately 45% of global production. The industrial sector faces a new energetic paradigm where distributed generation provided by small renewable energy sources may reduce the dependence from fossil energy sources as well as avoid energy distribution losses. Photovoltaic self-consumption systems can play an important role in confronting this challenge due to their modularity and their decreasing cost. Most of self-sufficiency energy studies are focused on building sector and discussions about the idiosyncrasy of industrial load profiles, and their matching capability with photovoltaic generation profiles can be scarcely found. This work analyzes the potential of photovoltaic self-consumption systems as a function of the array power, array tilt, and orientation angles to face the electric consumption in olive mills. Different recording intervals and reporting periods are considered. Results show that a self-sufficiency index of 40% may be achieved on olive harvest basis. Moreover, due to the load profile particularities, percentage error lower than 1.6% has been found when considering a recording interval of 60 min when matching the olive load consumption and photovoltaic generation profiles. Chosen array tilt and orientation angles may be key parameters to maximize the self-sufficiency index.

Keywords: Olive mill; photovoltaic; self-sufficiency; self-consumption

1. Introduction

World electricity generation from renewable energy is expected to considerably increase in the coming years, where wind and photovoltaics may constitute 29% and 40%, respectively, in world electricity generation by 2050 [1]. Currently, and due to its modularity and its decreasing cost, photovoltaic systems are very widespread: photovoltaic plants, building integration, stand-alone photovoltaic systems, water pumping, street lights, water desalination, space vehicles, satellites, and agriculture [2]. Regarding the agriculture sector, photovoltaic systems are used in different applications [3,4] such as dairy farms [5], wineries [6], agriculture in sea [7], olive mills [8], etc.

Olive mills are very extensive in the Mediterranean Basin, and Spain provides approximately 50% of European production and 45% of global production [9]. There are more than 2,000,000 hectares of olive trees in Spain and 28% of these hectare are irrigated [10]. More than 1700 olive mills are found in Spain, which produce more than 1,000,000 tons of olive oil per year according to the Agencia de Información y Control Alimentarios (AICA) [11,12].

The international olive oil market has undergone significant increase in levels of competition, where cost reduction strategies could improve competitiveness. In this scenario, direct photovoltaic self-consumption systems could promote energy self-sufficient mills, where energy cost and CO₂ emissions could be reduced [8].

Olive mills can be categorized regarding their production of olive oil. Large olive mills show an annual olive oil production higher than 5000 tons and an annual average electricity consumption around 923 MWh. Medium olive mills provide an olive oil production between 1000 and 5000 tons and show an average electricity consumption of 435 MWh. Finally, in small mills the olive oil production is lower than 1000 tons and average electrical consumption is 92 MWh [12], Table 1.

Table 1. Classification according to final olive oil production [12].

Categories	Olive Oil Production (t)	Average Electricity Consumption (MWh)
Small	<1000	92
Medium	1000 < production < 5000	435
Large	>5000	923

The electricity consumed by olive mills is obtained from the electricity grid. Electricity energy is used for different applications; see Table 2. There is energy consumption during a full year due to ancillary requirements, such as air compressors, computer systems, lighting systems, etc. However, there is equipment which is only used during the harvest period and it is used in various stages of olive oil processing, such as cleaning and crushing the olives. Motor drives of conveyor belts, washing for olives, destemmers, grinding, and mixing equipment centrifugal pumps consume the highest electrical energy. In this sense, two differentiated energy consumption periods can be found: no harvest, and harvest periods where the latter has a considerably higher load consumption.

Table 2. Classification according load consumption periods.

Category	Period	Electricity Consumption (MWh)
Harvest	December to March	Cleaning and crushing the olives. Motor drives of conveyor belts, washings for olive, destemmers, grinding and mixing equipment centrifugal pumps Applications ancillary, such as air compressors, computer systems, lighting system
Annual	Full year	Applications ancillary, such as air compressors, computer systems, lighting system

In Thailand a 50 kWp solar photovoltaic system may generate more than 75% energy due to different array tilt angles (β) and array orientation angles (α) [13]. Meanwhile, when tilt angle is fixed, almost 20% difference of generated energy from roof-integrated solar photovoltaic system was found when different orientation angles, $+2^\circ$ and -87° , were considered in the United Kingdom [14]. Several methods to search the optimum tilt and orientation angles in a fixed position at a specific location can be found [15–22]. The optimum orientation is usually suggested to be south-facing in the northern hemisphere and tilt angle is a function of the local latitude [23]. However, these methods are focused on maximizing the incident irradiance in a fixed position at a specific location but not on maximizing the matching between load and photovoltaic generation profiles.

In the literature several publications address the analysis and design of photovoltaic self-consumption systems for residential buildings [24–33], local communities [34], and office buildings [35]. Regarding agricultural industries, there is a lack of studies that show how self-consumption and self-sufficiency indices are affected due to array tilt and orientation angles photovoltaic modules. Moreover, the influence of the recording time resolution of measured data to estimate the energy parameters is not discussed. The design of a photovoltaic system through techno-economic solutions provided by HOWER are only

analyzed and proposed [6,8]. In this sense, the aims of this paper are to analyze the idiosyncrasy of olive mills regarding load profiles and their matching capability with direct photovoltaic generation profiles and how the array tilt and orientation angles may influence the self-consumption and self-sufficiency indices. The potential of photovoltaic systems in this type of industry when facing its load consumption will be shown. It must be noted that this work deals with direct self-consumption systems without storage. Energy storage devices are experiencing growth, and there a great number of new innovations, such as a system which insets lithium accumulators into photovoltaic modules for building photovoltaic [36]. However, large-scale energy storage, as required in this type of industry, is not easily developed because of high capital cost and a lack of financing options and incentives [37].

The paper is organized as follows: Section 2 provides the measured and estimated data together with the methodology to plot the self-sufficiency and self-consumption curves. Section 3 shows how self-sufficiency index may be influenced by array tilt and orientation angles. Moreover, the effects of the recording interval on the estimation of photovoltaic energy which is directly consumed is discussed, taking into account the particularities of olive mill load profile. Finally, conclusions are drawn in Section 4.

2. Materials and Methods

2.1. Input Data: Irradiance Profiles

Unpredictable changes in photovoltaic energy generation can be incurred by irradiance fluctuations in short-term time scales [38]. Different time scales of irradiance data are used from annual values in pre-design to short-term values to evaluate the system performance. Monthly and annual Global Horizontal Irradiance (GHI) data may be adequate time resolutions to evaluate the solar resource in a given region [39–43]. However, this time resolution for irradiance may not be appropriate for performance analysis and simulations, although it may depend on the dynamics of the solar profile and the system under study [44]. Moreover, the viability analysis of a solar energy project could also be sensitive to the time resolution of irradiance data [45]. The effect of averaging irradiance time-series could have a higher impact depending on the parameter under study. Larger values of sampling interval will tend to underestimate variability, while smaller sampling intervals will increase the amount of data and the complexity of monitoring devices and management. In this sense, the influence of the recording period when matching the load consumption and photovoltaic generation profiles should be taken into account to choose a proper recording period.

The case presented here, irradiance data is going to be considered with a recording interval of one minute together and one hour for analyzing the influence of the recording time resolution of measured data in order to estimate the energy parameters. In-plane irradiance (G_i) with an array tilt of 50° and global horizontal irradiance (GHI) are sampled each second with a recording interval of one minute. The former array tilt angle is latitude angle plus 15° degrees as this one is recommended in photovoltaic stand-alone system when wintertime load is most critical one [46]. The meteorological station is located in Jaén (latitude: $37^\circ 47' 14.35''$ N and longitude: $3^\circ 46' 39.73''$ W) and the thermopiles are classified as secondary standards according to ISO 9060. The measurement campaign was developed from April 2018 to March 2019.

The optimal array tilt angle depends on geographic latitude; however, in photovoltaic systems this angle and orientation may depend on the relationship between photovoltaic generation and electrical load demand [15–17,47]. In this sense, a Typical Meteorological Year (TMY) with different tilts (from 0° to 90° at 5° step) and facings (from -90° , west-facing, to $+90^\circ$, east facing with values of -90 , -60 , -30 , -20 , -10 , 0 , 10 , 20 , 30 , 60 , and 90°) have been obtained from Andalusian Energy Agency databases [48]. The provided data are obtained from measured parameters at ground stations and satellite images. The databases are hourly based and they may be used to study the influence of array tilt and orientation angles in self-consumption and self-sufficiency indices. In this sense, the array tilt and orientation angles for direct photovoltaic self-consumption systems for olive mills may be optimized according to

matching capability between load and irradiance profiles, which will maximize the self-sufficiency index and minimize the peak power of the photovoltaic system.

2.2. The Photovoltaic Generation Profile.

Different methods to estimate the output power of a solar photovoltaic system and the annual energy harvested by a photovoltaic system are summarized by Rus-Casas et al. [49]. Among the possible ways of estimating the output power, one of the simplest is the method based on the Performance Ratio (PR). The performance ratio indicates the overall effect of different losses on the output system due to array temperature and system component inefficiencies of failures, including balance of system components [50]. Moreover, this method is used in different works [51–54]. PR for conventional photovoltaic systems may be typically in a range from 0.70 to 0.80 in Spain [55]. In this paper, PR values of 0.75 will be considered, based on the experience of this kind of system [56–60]. In addition, if temperature is included as input parameter, the Standard Test Conditions Performance Ratio (PR'STC) could be used. PR'STC is calculated by adjusting the power rating at each recording interval to compensate the temperature difference between STC reference module temperature and the module temperature at that recording interval [50]. The output power may be estimated as:

$$P_{PVgen,\tau} = P_0 \times \frac{G_{i,k}}{G_{STC}} \times \left(1 + \gamma \times (T_{mod,k} - 25)\right) \times PR'STC \quad (1)$$

where $G_{i,k}$ (kWh/(m²)) corresponds to the global irradiation in time interval k, G_{STC} the global irradiance at Standard Test Conditions (1 kW/m²), γ is the relative maximum-power temperature coefficient (in units of °C⁻¹), γ has a value of 0.0035 °C⁻¹ for c.SI. $T_{mod,k}$ is the module temperature (in °C) in time interval k and it can be estimated as [60,61]:

$$T_{mod,k} = T_{amb} + G_{i,k} \times \frac{T_{NOCT} - 20}{800} - \frac{G}{G_{STC}} \times \Delta T \quad (2)$$

where ΔT for glass/cell/glass and for glass–cell–tedlar is 2 °C and 3 °C, respectively. T_{NOCT} is the nominal operating cell temperature.

There are several energy losses which are taken into account, such as angular, spectral, tolerance, and degradation, shading, dirt, dust, mismatch, etc. [49,62]. However, energy production could also be affected by the mounting structure, where free-standing photovoltaic systems could generate up to 5% more annual energy than roof-integrated photovoltaic systems in hot climates. In cold, moderate, and warm climates, the annual energy may be reduced from 3% to 4% [63]. Therefore, this lost energy should be also taken into account when photovoltaic systems are designed, as olive mills usually provide large spaces on the roofs and yards where photovoltaic systems could be installed.

The PV generation profiles have been estimated considering either measured irradiance and ambient temperature data or the TMY database.

The photovoltaic generator has been evaluated considering a range of peak power, P_0 , from 0.01 to 1000kWp with an increase step of 10 kWp.

2.3. Input Data: Load Consumption Profile

The electrical load profile was monitored though a year in an olive mill which manages the milling, packaging, and storage processes. A smart meter was used to measure the active and reactive energy with a recording interval of 15 min, which may be appropriate for either monthly or annual reporting periods [64]. The measurement campaign was developed from April 2018 to March 2019. As shown in Table 3, the electricity consumption is 1407 MWh/year; therefore the olive mill can be categorized as a large one and the olive oil production is 5600 tons per year.

Table 3. Olive mill load consumption.

Period	Monitoring Period (Year)	Electricity Consumption (kWh/Period)			Daylight/Total (%)	Monthly/Year (%)	Monthly/Year (%) (Daylight Hours)
		Total Hours	Daylight Hours	Night Hours			
January	2019	233352.0	91334.9	142017.1	39.1	16.6	13.4
February	2019	208175.0	92891.8	115283.2	44.6	14.8	13.6
March	2019	139263.0	79591.3	59671.7	57.2	9.9	11.7
April	2018	107102.0	60758.1	46343.9	56.7	7.6	8.9
May	2018	75133.0	50591.8	24541.2	67.3	5.3	7.4
June	2018	68283.0	43612.9	24670.1	63.9	4.9	6.4
July	2018	64509.0	45226.5	19282.5	70.1	4.6	6.6
August	2018	67635.0	38276.9	29358.1	56.6	4.8	5.6
September	2018	52970.0	27188.5	25781.5	51.3	3.8	4.0
October	2018	67194.0	27944.7	39249.3	41.6	4.8	4.1
November	2018	125344.0	47475.7	77868.3	37.9	8.9	7.0
December	2018	198244.0	77012.8	121231.2	38.8	14.1	11.3
Year	2018	1407204.0	681905.8	725298.2			

In Table 3, electricity consumption is classified depending on time basis: total hours (24 h), daylight hours (from sunrise to sunset), and night hours (from sunset to sunrise). Daylight and night hours are estimated through an astronomical model which shows when sunrise and sunset occur [65]. Moreover, this table gives different ratios: the ratio of electricity consumption throughout daylight hours to electricity consumption throughout total hours (Equation (3)); the ratio of electricity consumption for a whole month to electricity consumption for the whole year (Equation (4)); and the ratio of electricity consumption for a month throughout daylight hours to electricity consumption for the whole year throughout daylight hours (Equation (5)):

$$\frac{\text{Daylight}}{\text{Total}} = \frac{E_{L,d,ss}}{E_{L,d}} \quad (3)$$

$$\frac{\text{Monthly}}{\text{Year}} = \frac{E_{L,m}}{E_{L,y}} \quad (4)$$

$$\frac{\text{Monthly}}{\text{Year}}(\text{daylight hours}) = \frac{E_{L,m,ss}}{E_{L,y,ss}} \quad (5)$$

where $E_{L,d,ss}$ is the electricity consumption throughout daylight hours; $E_{L,d}$ is the electricity consumption throughout the whole day; $E_{L,m}$ is the electricity consumption for a whole month; $E_{L,y}$ is the electricity consumption for the whole year; $E_{L,m,ss}$ is the electricity consumption for a month throughout daylight hours and $E_{L,y,ss}$ is the electricity consumption for the whole year throughout daylight hours.

During the four months which generally correspond to olive harvest (i.e., December, January, February, and March) the monthly power consumption is higher (>9.9% of the annual consumption) than the rest of the months. In November “early harvest” takes place to obtain the virgin extra olive oil (premium product) and the monthly load consumption is slightly lower than 9% of the total load consumption. Furthermore, the electrical consumption is high in April (7.6%) as this month is a transition month that can be considered as a harvest month depending on the environmental conditions and the production of olives. During this month, there is a packaging process in the olive mill. The rest of the months, from May to October, there is a considerably lower power consumption. It must be noted that during the months of olive harvest, the power consumption from sunrise to sunset is lower than the rest of the months. In this period, the number of daylight hours are lower than night hours.

However, from December to March the percentage of power consumption during daylight hours is 50% of energy consumption year during daylight hours. Therefore, two clearly differentiated periods regarding consumption may be found: olive harvest and no olive harvest.

2.4. Photovoltaic Energy Consumed, Self-Consumption, and Self-Sufficiency Indices.

A photovoltaic self-consumption system can be evaluated by self-consumption and self-sufficiency indices, Φ_{sc} and Φ_{ss} , respectively, together with energy parameters, such as the photovoltaic generated energy which is directly consumed, $E_{PV,con}$ [28]. The latter is estimated from olive mill load consumption data, E_L , and photovoltaic generated energy data, $E_{PV,gen}$, using Equation (6) [51,52]. $E_{PV,con,k,\tau k}$ corresponds to $E_{L,k,\tau k}$ when $E_{L,k,\tau k}$ is lower than $E_{PV,gen,k,\tau k}$. Meanwhile, $E_{PV,con,k,\tau k}$ coincides with $E_{PV,gen,k,\tau k}$ when $E_{L,k,\tau k}$ is higher than $E_{PV,gen,k,\tau k}$.

$$E_{PV,con,k,\tau k} = \begin{cases} E_{L,k,\tau k} & \text{if } E_{PV,gen,k,\tau k} \geq E_{L,k,\tau k} \\ E_{PV,gen,k,\tau k} & \text{if } E_{PV,gen,k,\tau k} < E_{L,k,\tau k} \end{cases} \quad (6)$$

where τ_k is the duration of the k_{th} recording interval within a reporting period and k is the number of recording intervals in the reporting period [50].

The aforementioned parameters may be calculated in a given reporting period (monthly, olive harvest period, and annual) through Equations (7)–(9):

$$E_{PV,gen,\tau} = \sum_k P_{PV,gen,k,\tau k} \times \tau_k \quad (7)$$

$$E_{L,\tau} = \sum_k P_{L,k,\tau k} \times \tau_k \quad (8)$$

$$E_{PV,con,\tau} = \sum_k P_{PV,con,k,\tau k} \times \tau_k \quad (9)$$

where τ denotes the reporting period.

The self-consumption index, Φ_{sc} , can be defined as the percentage of $E_{PV,gen}$ which is locally consumed (Equation (10)). On the other hand, the self-sufficiency index, Φ_{ss} , provides the percentage of E_L which is consumed over a reporting period from photovoltaic generated energy (Equation (11)) [66]

$$\Phi_{sc,\tau} = \frac{E_{PV,con,\tau}}{E_{PV,gen,\tau}} \quad (10)$$

$$\Phi_{ss,\tau} = \frac{E_{PV,con,\tau}}{E_{L,\tau}} \quad (11)$$

Self-consumption and self-sufficiency indices can be plotted as function of array peak power [51], Figure 1.

2.5. Effect of Averaging Irradiance Time-Series in Photovoltaic Direct Self-Consumption in Olive Mills

In this manuscript, direct photovoltaic energy consumed is estimated considering two recording intervals, 15 min and 60 min, where 15 min recording interval data have been selected as reference data. The irradiance data, which are measured by the meteorological station with a recording interval of one minute, are averaged every 15 min to have the same recording interval as E_L and $E_{PV,gen}$. Both recorded parameters (15 and 60 min) are used to analyze the error when matching the load consumption and photovoltaic profiles in a photovoltaic direct self-consumption system. If low errors are obtained, hourly irradiance data provided by TMY database may be used to study the influence of array tilt and orientation angles on the self-consumption and self-sufficiency indices for the olive mill under study.

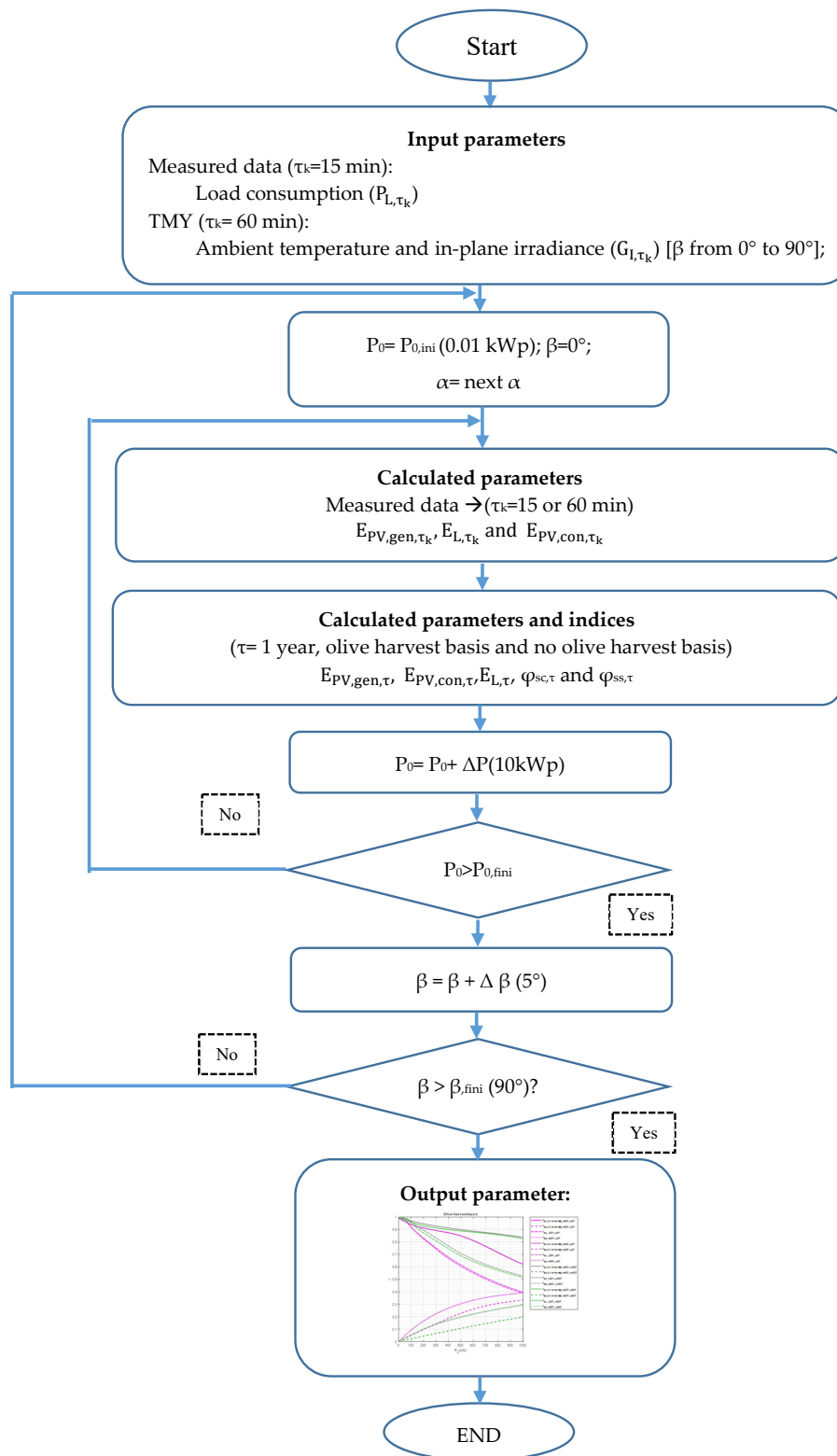


Figure 1. How to plot Φ_{sc} and Φ_{ss} as a function of the nominal array power, P_0 [51,52,64].

The percentage error (PE) when analyzing the matching capability due to different recording intervals may be expressed as [64,66–69]:

$$PE = \frac{X_{estimated} - X_{ref}}{X_{ref}} \tag{12}$$

where X represents the parameter considered.

PE can be plotted as function of array peak power, Figure 2.

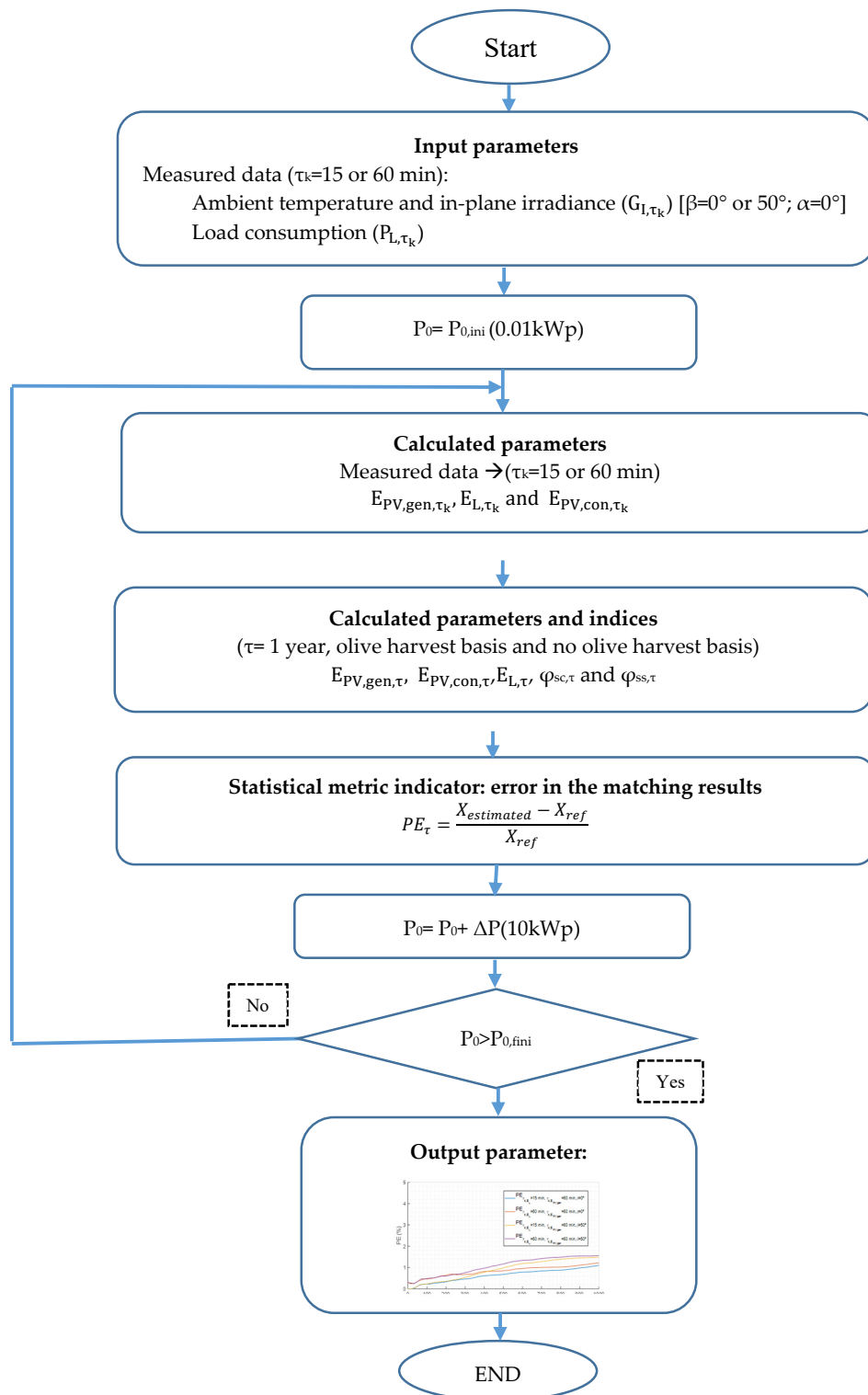


Figure 2. How to estimate the percentage error as function of the nominal array power, P_0 [51,52,64].

where $P_{0,fini}$ corresponds to 1000 kWp and β_{fini} has a value of 90° .

3. Results and Discussion

3.1. Impact of Recording Time in Self-Consumption Analysis

To provide a proper analysis, it is necessary to accurately know the irradiance and the load consumption profiles [70–73]. In this sense, the annual percentage error for $E_{PV,con}$ is estimated when a recording interval of 60 min of $E_{PV,gen}$ and E_L is used instead of 15 min on an annual basis, as shown in Figure 3. As can be seen in this figure, annual PEs provide values lower than 1.6% when a recording interval of 60 min is considered. These small values of PE may be due to the shape of olive mills load profile: it is almost constant with a low variability during the daylight hours and the load profile is generally above the generation curves when P_0 has a value lower than 200 kW_p, as can be seen in Figure 4. This figure represents a harvest day with two different array powers, P_0 (200 kW_p and 500kW_p) and different recording intervals (15 min and 60 min).

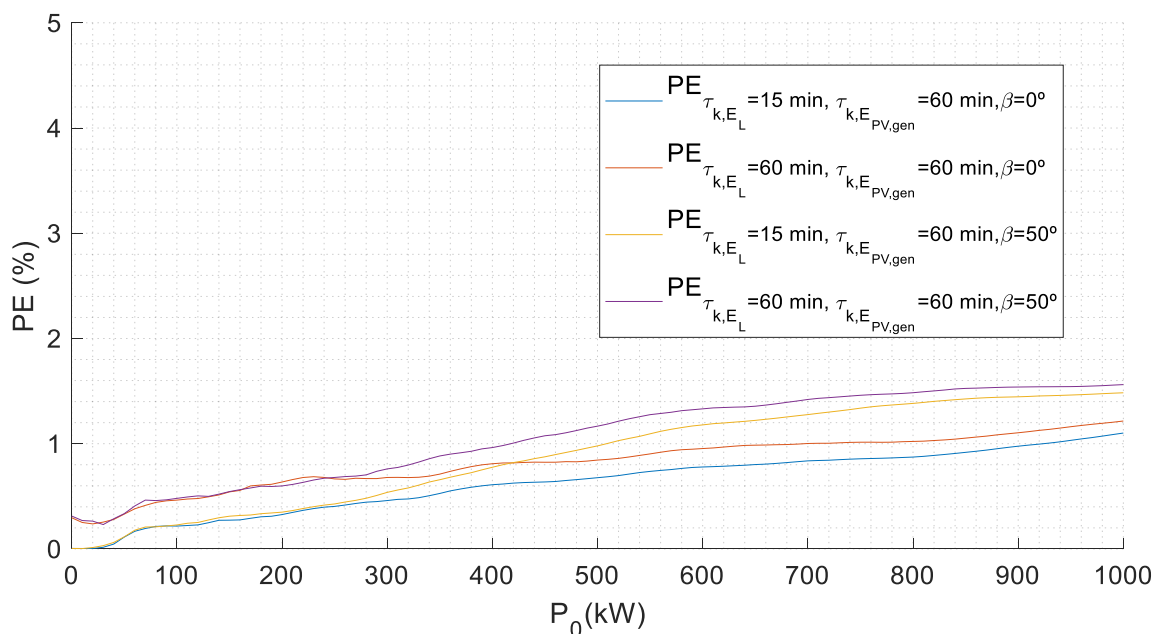


Figure 3. Annual self-consumed photovoltaic energy error as a function of P_0 considering a recording interval of 60 min. Recording interval of 15 min either for $E_{PV,gen}$ and E_L has been taken as a reference when $E_{PV,con}$ is estimated.

Although it may be desirable to use a recording interval as short as possible [64,66], the impact on the self-consumption analysis may depend on the dynamics of the solar profile and the system under study [44]. Therefore, the error when matching the olive mill load consumption profile and photovoltaic generation profiles in a photovoltaic direct self-consumption system with a recording period of 60 min may be considerably lower than the ones observed in residential buildings [64,66–69,74–76]. Therefore, hourly irradiance data and a recording interval of 15 min for E_L may be used to estimate $E_{PV,con}$, Φ_{sc} and Φ_{ss} in this type of industries on an annual basis.

3.2. Influence of Array Tilt and Orientation Angles in Self-Consumption and Self-Sufficiency Indices.

Photovoltaic generation profiles have been estimated considering different combinations of array tilt angle, from 0° to 90° at 5° increments, and orientation angles from -90° to 90° , where $\alpha = 0^\circ$ corresponds to south. Array powers (P_0) range between 0.01 kW_p to 1000 kW_p at 10 kW_p step. Each one of these 21109 photovoltaic generation profiles, together with the olive mill load profile have been used to calculate the self-consumption and self-sufficiency indices on an annual basis, on an olive

harvest basis and on a no olive harvest basis. This work considers olive harvest period from December to March; therefore, from April to November may be considered to be no harvest period.

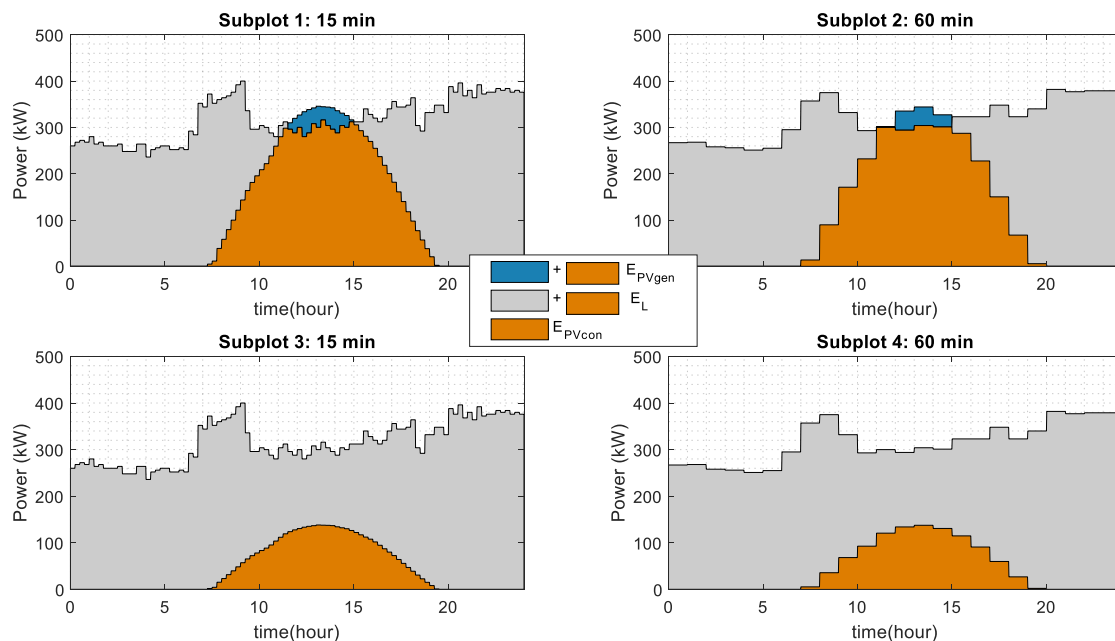
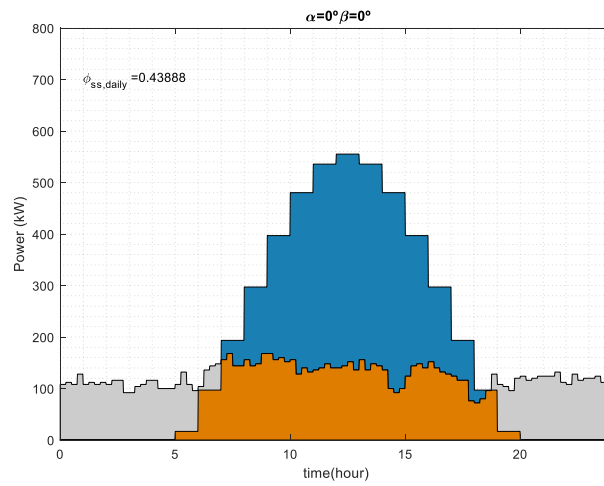
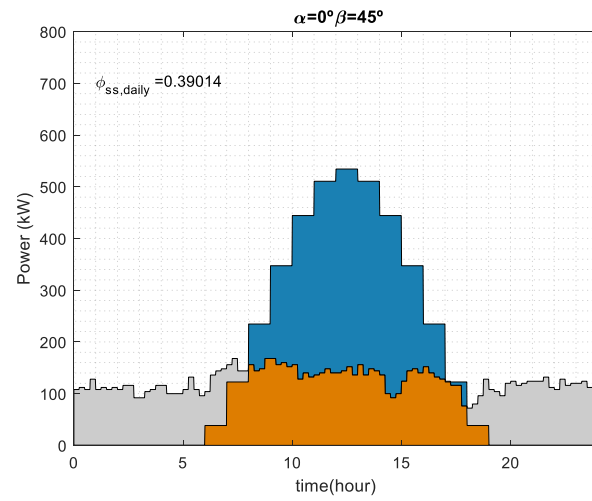


Figure 4. Daily photovoltaic generation and load consumption of an olive mill in Jaén (South of Spain). Load and Irradiance data correspond to 27 March 2019. $E_{PV,con}$ is represented by the orange area, $E_{PV,gen}$ is given by blue and orange area and E_L is represented by grey and orange areas. In Subplots 1 and 2 the array power considered, P_0 , is 500 kW_p, meanwhile Subplots 3 and 4 corresponds to array power of 200kW_p. The recording interval is 15 min in Subplots 1 and 3; on the other hand, Subplots 2 and 4 has a 60 min recording interval. Orientation angle and tilt angle have a value of 0°.

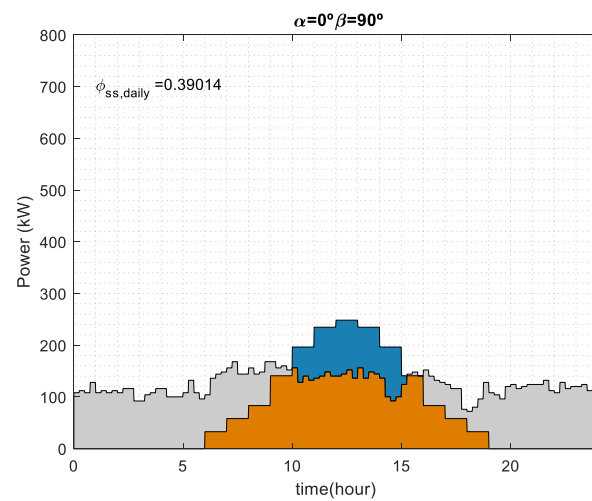
Figure 5 shows a no harvest day for three different orientation angles, 0°, −90°, and 90°, and three array tilt angles, 0°, 45°, and 90°. As can be seen, the different photovoltaic generator profiles may vary the self-sufficiency index from 0.39 to 0.44. For $\alpha = 0^\circ$ the photovoltaic self-consumption energy is maximized at noon, Subplots 1, 2, and 3. However, in Subplots 4 and 5 for $\alpha = -90^\circ$ the self-consumption energy is emphasized in the morning. Meanwhile, in Subplots 6 and 7 for $\alpha = 90^\circ$ the photovoltaic generation is higher in the afternoon. Although the self-sufficiency indices are quite similar for the seven analyzed cases, the poorest result is obtained when south-facing and $\beta = 45^\circ$ and 90° are considered. It must be noted that 45° is the array tilt and the south-facing of orientation angles may be considered the optimum ones when the annual photovoltaic energy generation must be maximized [15–17]. This fact emphasizes the need for photovoltaic self-consumption analysis for a given load profile to find not only the optimum array energy generation but the tilt and orientation angles which maximize the matching capability.



Subplot 1

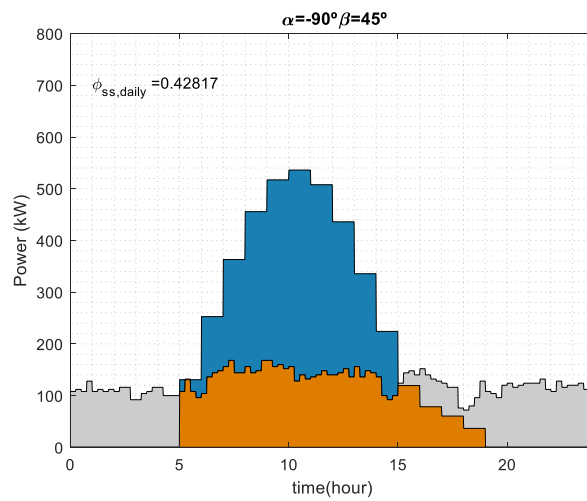


Subplot 2

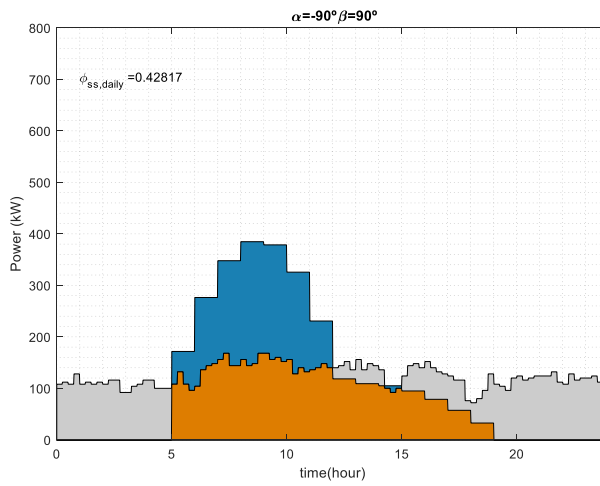


Subplot 3

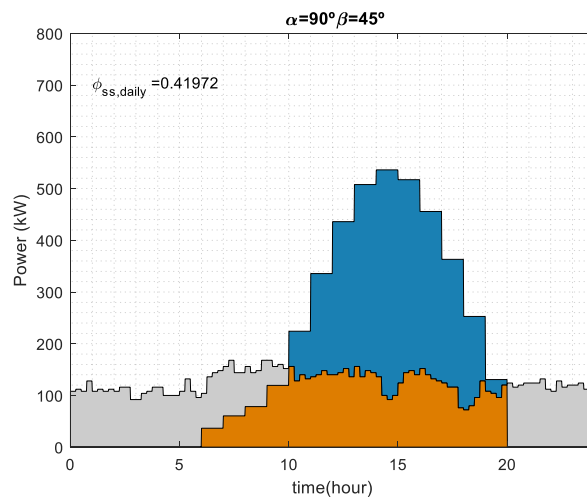
Figure 5. Cont.



Subplot 4



Subplot 5



Subplot 6

Figure 5. Cont.

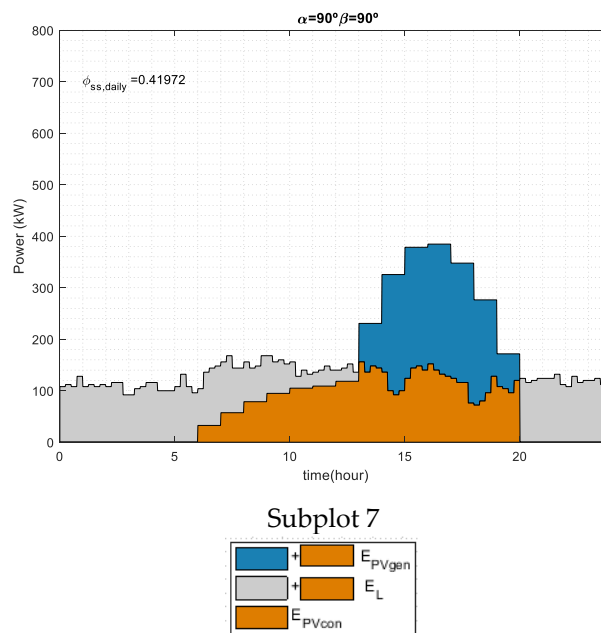


Figure 5. Daily photovoltaic generation and load consumption of olive mill in Jaén (South of Spain). Load data correspond to 3 June 2018 and irradiance data correspond to 3 June TMY. $E_{PV,con}$ is represented by the orange area while $E_{PV,gen}$ is given by blue and orange area and E_L is represented by grey and orange areas. P_0 is 900 kW_p and the recording interval is 15 min for load profile and 60 min for photovoltaic generator profile. Subplot 1: $\alpha = 0^\circ$ and $\beta = 0^\circ$, Subplot 2: $\alpha = 0^\circ$ and $\beta = 45^\circ$, Subplot 3: $\alpha = 0^\circ$ and $\beta = 90^\circ$, Subplot 4: $\alpha = -90^\circ$ and $\beta = 45^\circ$, Subplot 5: $\alpha = -90^\circ$ and $\beta = 90^\circ$, Subplot 6: $\alpha = 90^\circ$ and $\beta = 45^\circ$ and Subplot 7: $\alpha = 90^\circ$ and $\beta = 90^\circ$.

Table 4 shows the array tilt and orientation angles which maximize and minimize the self-sufficiency index for each peak power on an annual basis, an olive harvest basis, and no olive harvest basis, respectively. As can be seen in Table 4, for an annual basis, the orientation angles which maximize Φ_{ss} are south-facing (0°) for P_0 between 0.01 and 140 kW_p and -10° for P_0 higher than 140 kW_p. Meanwhile, the array tilt angles that provide the best self-sufficiency index are between 30° and 45° , depending on P_0 . On the other hand, when an olive harvest basis is considered, the best results are obtained with array tilt angles that range from 50° and 55° and the orientation angle is 0° , Table 4. As can be seen, higher array tilt angles are needed on an olive harvest basis than on an annual basis. Olive harvest periods are months where the solar elevation is lower than no olive harvest period. Therefore, to maximize the generated photovoltaic energy during olive harvest period, higher array tilt angles from 50° to 55° are needed. As the photovoltaic energy generation must be maximized in winter months, the array tilt must be considerably increased as is the case of photovoltaic stand-alone systems. The recommended array tilt angle for this type of system will be chosen to meet the load in the worst month. In this way, for a fixed orientation angle, tilt angle should be set at the latitude angle plus 15° degrees when wintertime load is the most critical and latitude angle minus 15° degrees when summertime load is the most critical [46]. The former may correspond to olive mills as the high consumption and the less generation is achieved in winter months.

If a no olive harvest basis is considered, the array tilt angles that provide the best Φ_{ss} may range from 0° to 20° and the orientation angles may vary from -30° to 0° and 90° . The array tilt angles are lower than the ones obtained on an annual basis and an olive harvest basis. It must be noted that this period corresponds to months where the sun is relatively high in the sky so the tilt angle must be low to maximize the collected energy. However, when P_0 is larger than 600 kW_p, the orientation angle needs to maximize self-sufficiency index, thus having a value of 90° . On the other hand, Φ_{ss} has a minimum value when array tilt angle is 90° for most cases. Vertical façade is used in building-integrated photovoltaics (BIPV); however not only a significant impact on the annual energy output of BIPV

system may be found due tilt and orientation angles [77], but also self-sufficiency index may be 25% lower as shown in Figure 5.

Table 4. Maximum and minimum self-sufficiency indices as a function of P_0 .

Reporting Period	Φ_{ss}	β (°)	α (°)	P_0 (kW _p)	
Annual basis	Max	30	0	[0.01–110]	
		35	0	[110–140]	
		35	–10	[140–300]	
		40	–10	[300–690]	
		45	–10	[690–820]	
		40	–10	[820–1000]	
	Min	90	–90	[0.01–60]	
		90	90	[60–1000]	
	Olive harvest basis	Max	50	0	[0.01–70]
			55	0	[70–1000]
Min		90	–90	[0.01–20]	
		90	90	[20–1000]	
No olive harvest basis	Max	25	0	[0.01–170]	
		20	0	[170–310]	
		20	–10	[310–380]	
		20	–30	[380–400]	
		15	–30	[400–490]	
		10	–30	[490–600]	
		0	90	[600–1000]	
	Min	90	0	[0.01–120]	
		90	90	[120–1000]	

As has been seen, Φ_{ss} is influenced by array tilt and orientation angles and the angles which maximizes and minimizes Φ_{ss} also depends on P_0 . Once the maximum and minimum Φ_{ss} are defined, the self-sufficiency and self-consumption indices as function of P_0 will be plotted. Only curves, which maximize and minimize the self-sufficiency index, are provided. The rest of the curves are within these limits.

Figures 6–8 represent the self-consumption and self-sufficiency indices as a function of the nominal array power, which have been obtained through the photovoltaic generation and olive mill profile matchings. As has been aforementioned, the array tilt and orientation angles that maximize and minimize the self-sufficiency indices have been considered. As can be seen in Figures 6 and 7, when P_0 is higher than 300 kW_p, $\Phi_{ss, \max}$ and $\Phi_{ss, \min}$ may vary up to 25%; however, the difference between $\Phi_{ss, \max}$ and $\Phi_{ss, \min}$ values are lower than 15% when P_0 is less than 300kW_p. $\Phi_{ss, \max}$ curves in Figure 8 shows a greater slope up to 400 kW_p. Therefore, the lower P_0 , the smaller influence of self-sufficiency index is due to array tilt and orientation angles. It must be noted that on an annual and olive harvest basis, especially in the latter, high self-consumption indices may be reached, i.e., a high matching capability is achieved.

It must be noted that self-sufficiency curves are asymptotic [51,52]. However, in this case, where a large olive mill is considered, and in order to see the asymptotes, unrealistic array powers (i.e., much higher than 1 MW) may be considered. In any case, it can be seen that either on annual or harvest basis, photovoltaic self-consumption without storage may provide self-sufficiency indices below 0.5, i.e., almost half the load consumption may be obtained direct from photovoltaics. On the other hand, on a no harvest basis the self-sufficiency index may be slightly higher than 0.5.

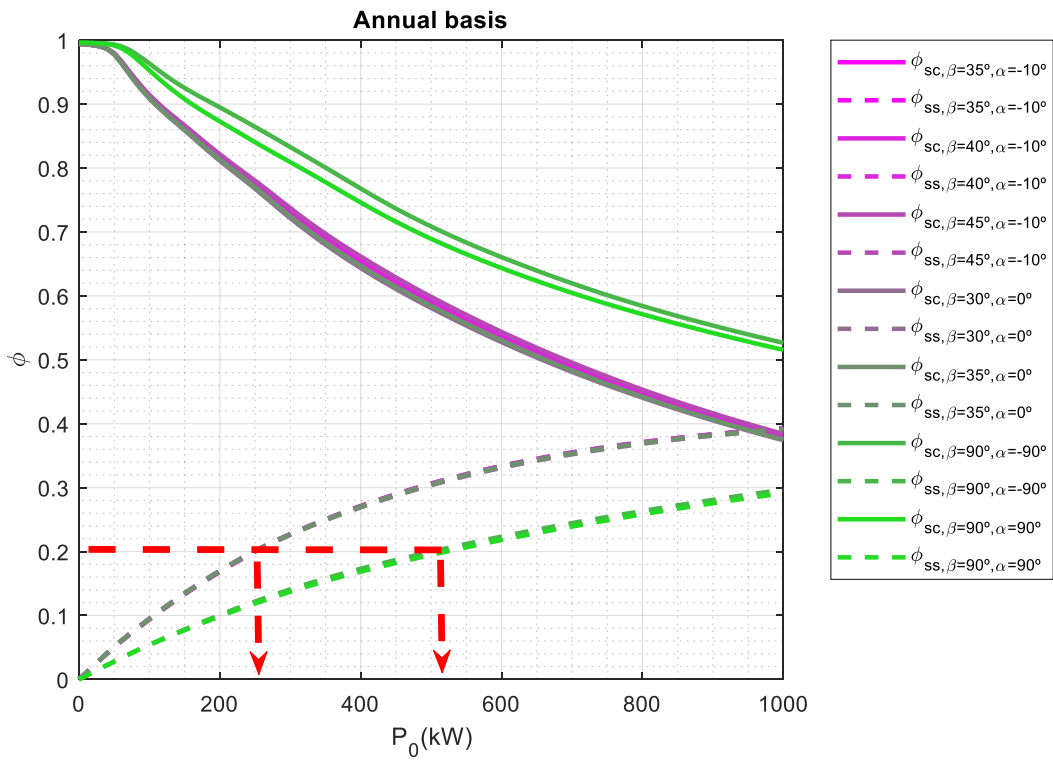


Figure 6. Annual basis. Φ_{sc} and Φ_{ss} curves which maximizes Φ_{ss} .

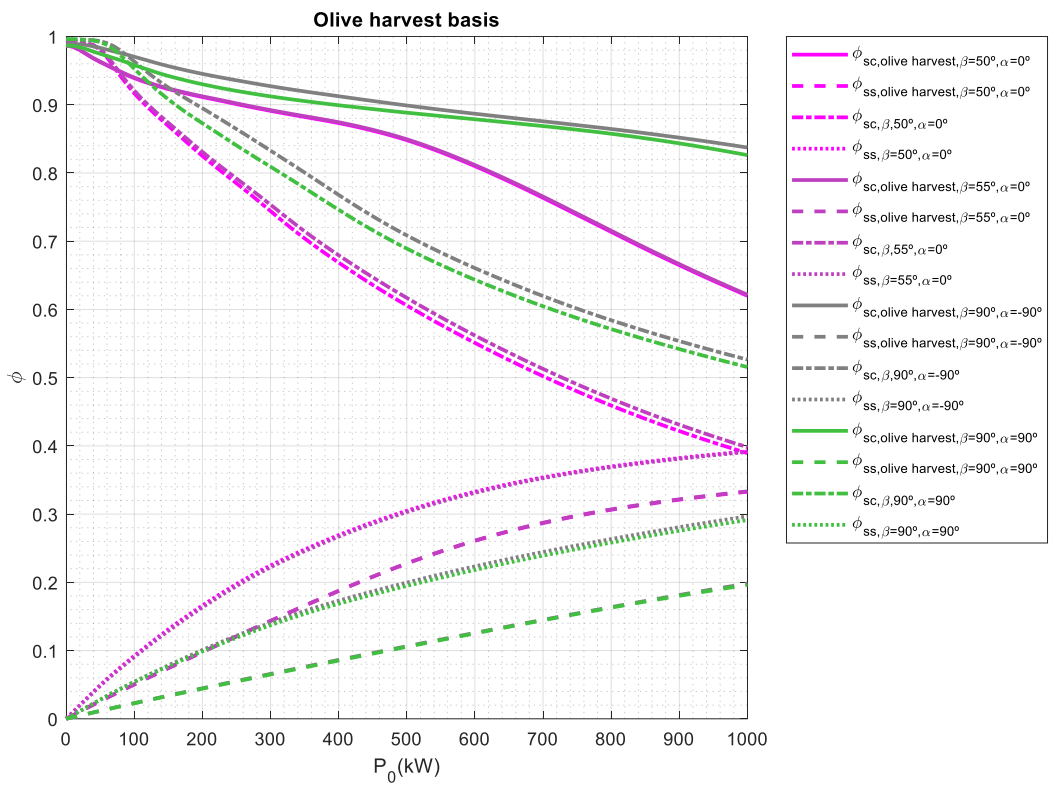


Figure 7. Olive harvest basis. Φ_{sc} and Φ_{ss} curves which maximizes and minimizes the Φ_{ss} .

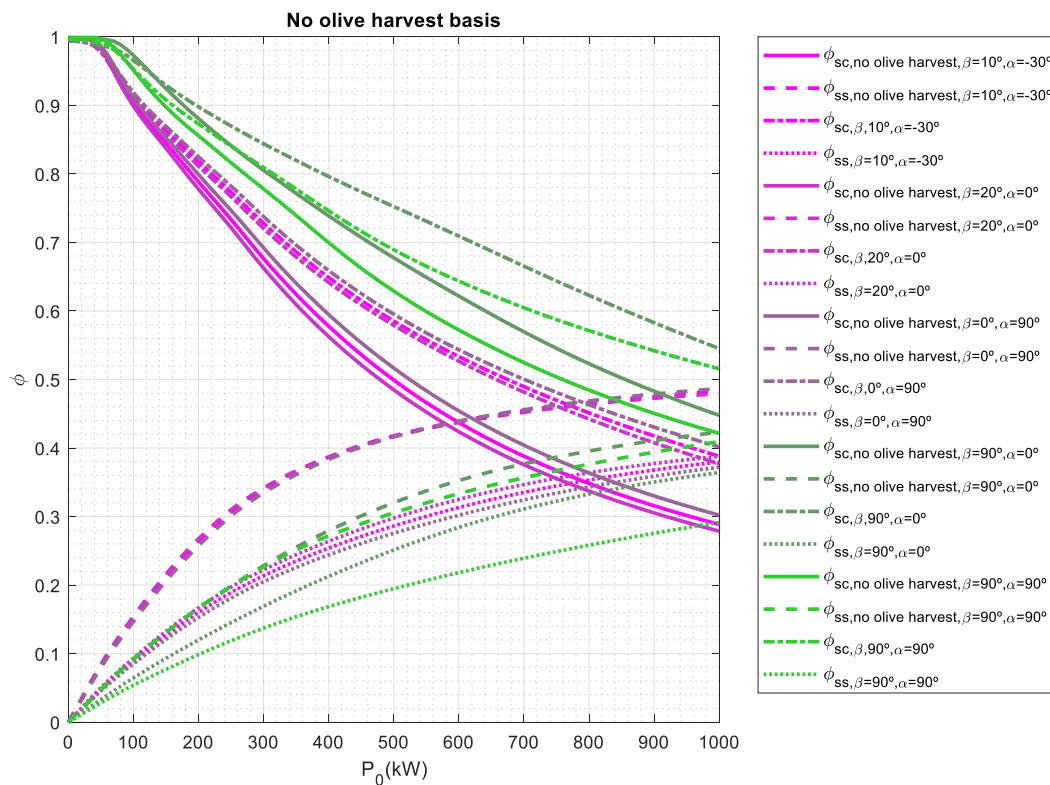


Figure 8. No harvest basis. Φ_{sc} and Φ_{ss} curves which maximizes and minimizes Φ_{ss} .

In Figure 6, array tilt and orientation angles may be used to optimize the photovoltaic generator, e.g., if a 0.2 annual self-sufficiency index must be achieved, the photovoltaic peak power may range from 250 kWp to 500 kWp and annual self-consumption index may vary from 0.78 to 0.7. Therefore, in this case, the peak power may be doubled to obtain the same Φ_{ss} . This highlights the influence of array tilt and orientation angles when maximizing photovoltaic energy consumed and self-sufficiency indices. Moreover, it must be noted the high self-consumption index that may be achieved which approaches 0.8. Figures 9–11 show the self-consumption and self-sufficiency curves for tilt and orientation angles, which maximize self-sufficiency index for photovoltaic generator of 250 kWp. These figures provide the indices in different periods: annual, harvest period, and no harvest period. In Table 5 is shown the values of both indices for annual, harvest period, and no harvest period when a 250 kWp array power is considered. Self-sufficiency indices are similar for 35°, 20°, and 55° with values in the range from 0.2 to 0.19 on an annual basis; however, Φ_{ss} for 90° is 0.11, only half of these values.

Figures 6–8 allow analysis of the range of array powers which provide a given self-sufficiency index from different basis (annual, olive harvest, and no olive harvest). Moreover, if peak power of photovoltaic generator is known, the range of self-consumption and self-sufficiency indices which may be obtained if array tilt and orientation angles are modified.

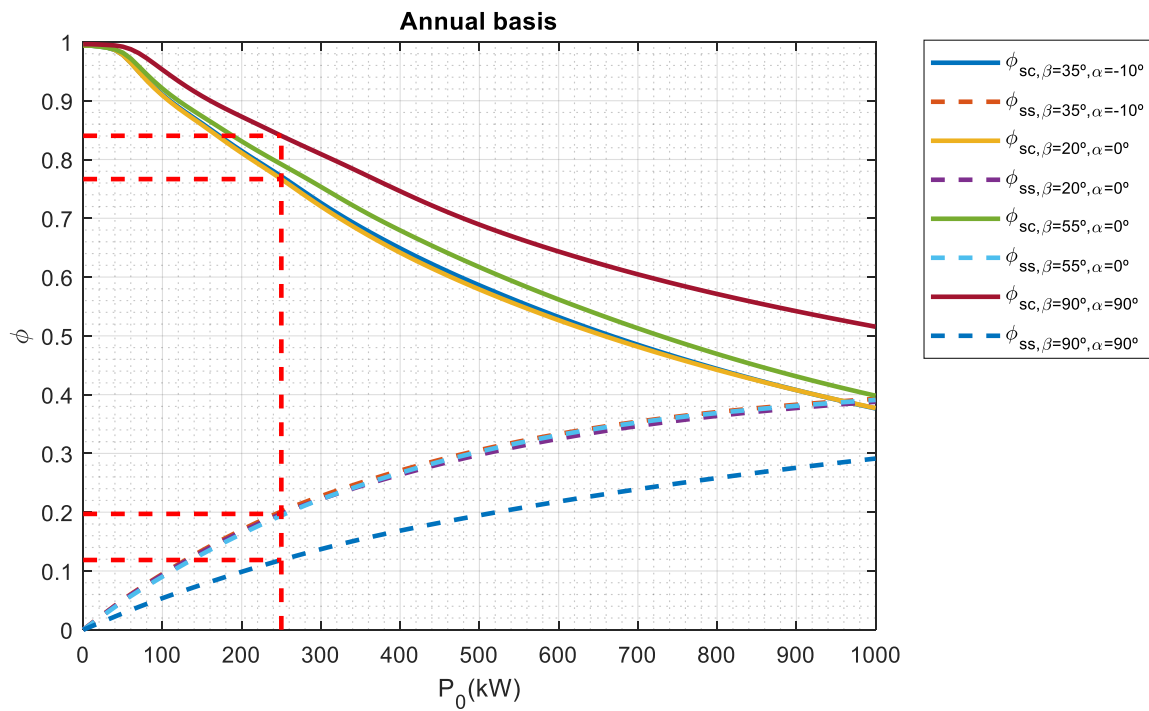


Figure 9. Annual basis. Self-consumption and self-sufficiency curves as a function of P_0 .

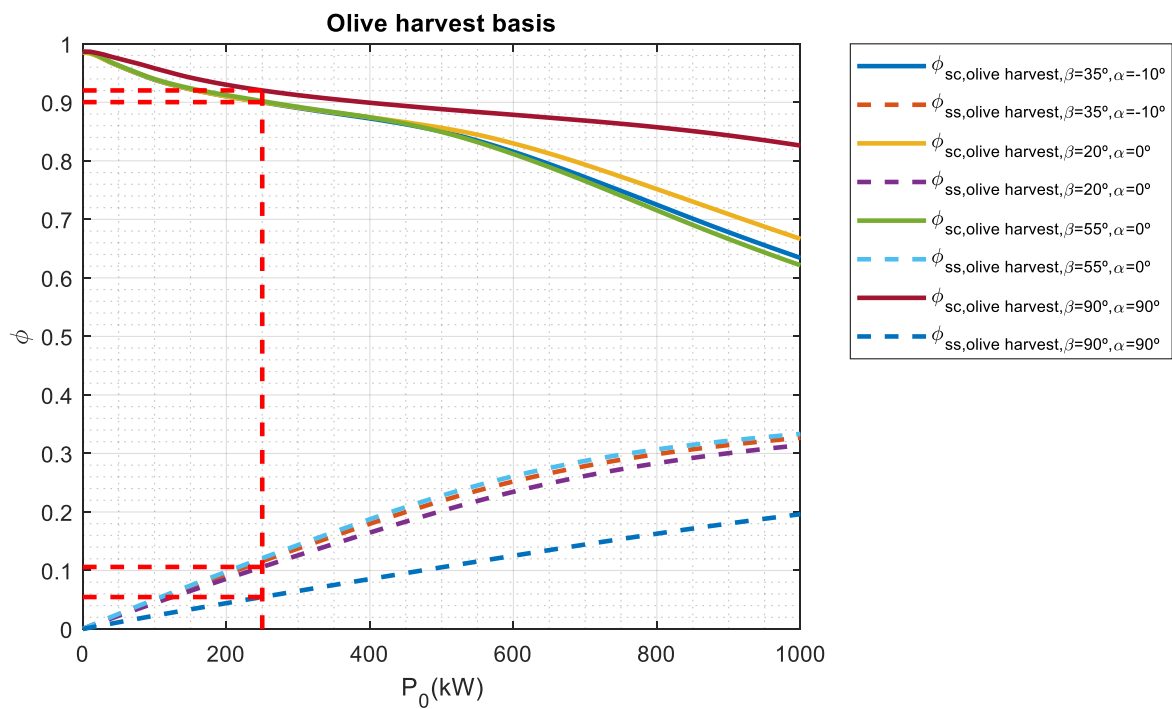


Figure 10. Olive harvest basis. Self-consumption and self-sufficiency curves as a function of P_0 .

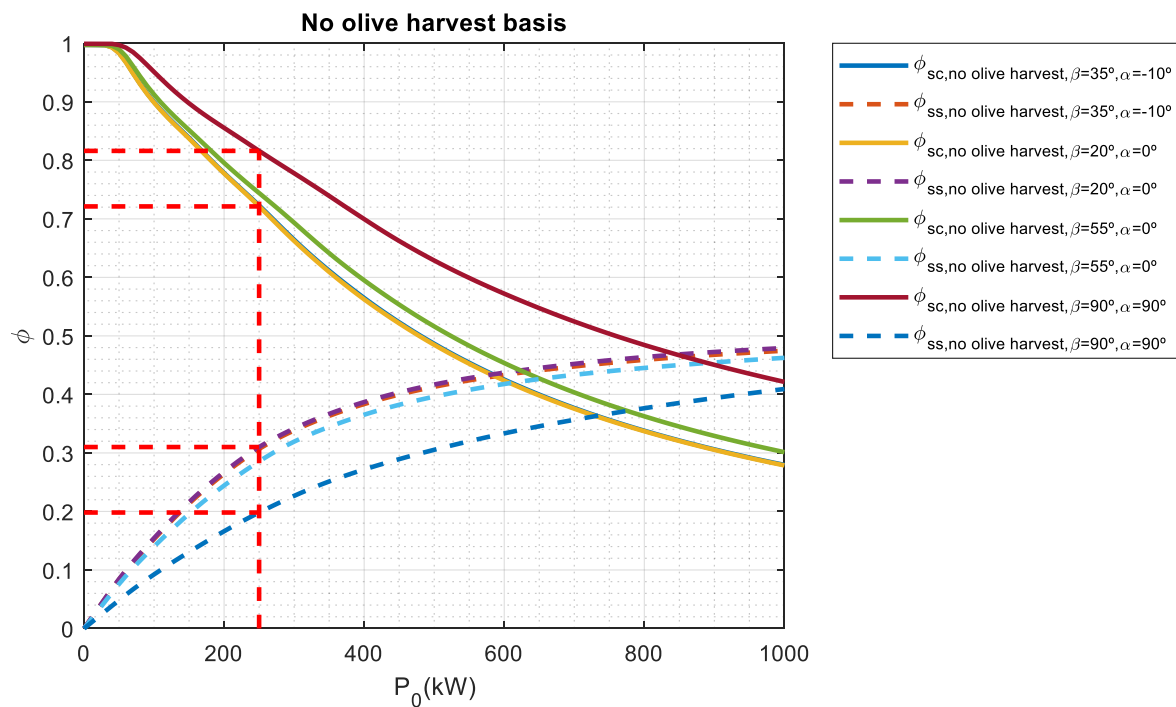


Figure 11. No harvest basis. Self-consumption and self-sufficiency curves as a function of P_0 .

Table 5. Self-consumption and self-sufficiency indices with $P_0 = 250$ kWp.

P_0 (kW _p)	β (°)	α (°)	Reporting Period	Φ_{sc}	Φ_{ss}
250	35	−10	Annual basis	0.7714	0.2012
			Olive harvest basis	0.9002	0.1159
			No olive harvest basis	0.7229	0.3069
	20	0	Annual basis	0.7667	0.1971
			Olive harvest basis	0.9004	0.1060
			No olive harvest basis	0.7212	0.3101
	55	0	Annual basis	0.7918	0.1944
			Olive harvest basis	0.9020	0.1209
			No olive harvest basis	0.7441	0.2855
	90	90	Annual basis	0.8404	0.1187
			Olive harvest basis	0.9203	0.0546
			No olive harvest basis	0.8161	0.1982

4. Conclusions

It has been shown that from an energetic point of view, photovoltaic self-consumption systems without storage may be suitable for olive mills. High self-consumption index may be achieved (>80%), which provides a high matching capability between load and consumption profiles, together with self-sufficiency index ranging from 20% to 30% for the olive harvest period (i.e., 20%–30% of the load consumption may be covered with direct self-consumption without storage and most of the photovoltaic generated energy is self-consumed by the olive mill). Self-sufficiency index values provided by this type of system in olive mills may be quite similar to or higher than the ones obtained in the residential sector.

In this paper, the impact of recording time when estimating photovoltaic self-consumption and self-sufficiency indices (Φ_{sc} and Φ_{ss}) in olive mills have been analyzed. Moreover, how these indices may be influenced by array tilt and orientation angles in this type of industry have been developed. It

must be highlighted that the results obtained here may be extrapolated to any industry with a load consumption profile with low variability during daylight hours.

As established, it is recommended that recording interval may be as short as possible, due to the impacts on the estimation of the self-consumed energy; higher recording intervals may provide an overestimation of $E_{PV_{con}}$. However, load consumption profile in an olive mill generally has low variations during sunshine hours. In this sense, it has been shown that regarding direct self-consumption (i.e., without storage) the error when matching the olive mill load consumption and photovoltaic generation profiles with a recording period of 60 min may be considerably lower than the ones observed in residential buildings. Percentage error lower than 1.6% has been found if a recording interval of 60 min is considered, when matching the olive load consumption and photovoltaic generation profiles. Therefore, hourly irradiance and load consumption data with a recording interval of 1 h may be used to estimate $E_{PV_{con}}$, Φ_{sc} , and Φ_{ss} in this type of industry from an annual basis. In this sense, data provided with such a recording interval may be used to analyze the performance of photovoltaic self-consumption systems in olive mills. Moreover, load data considering this time resolution may be used as long as the load consumption profiles shows little variability during photovoltaic generation. It must be highlighted that load consumption data with an hourly recording interval are generally provided by the grid operators, so a huge amount of data may be used to assess the potential of photovoltaic technology in olive mills.

Olive mill load profiles follow two fixed patterns through the year: olive harvest and no olive harvest periods. Olive harvest period is from December to March; although the period is only four months the energy consumption may be 50% of energy consumption during daylight hours.

Array tilt and orientation angles, which maximize self-sufficiency index, depend on P_0 . When annual basis is considered, self-sufficiency index may be maximized if array tilt angle varies from 30° to 45° and orientation angle from -10° to 0° . However, array tilt angle has a range from 50° to 55° and orientation angle is true south when olive harvest period is considered. Meanwhile, array tilt angle has a range from 0° to 25° and orientation angle is from -30° to 0° and 90° . Array tilt of 90° and orientation angle of east or west minimizes the value of self-sufficiency index in all range of P_0 and for the three periods: annual, olive harvest, and no olive harvest.

If a proper design of photovoltaic system is achieved, self-sufficiency index may range from 0.2 to 0.3 and self-consumption index may be relatively high within the range 0.6–0.8 for $P_0 = 250\text{--}500\text{kW}_p$.

Author Contributions: All authors (G.J.-C., F.J.M.-R., A.J.M.-C., G.M.T. and C.R.-C.) contributed equally to this work. All authors have read and agreed to the published version of the manuscript.

Funding: This research was funded by the Agencia Estatal de Investigación (AEI) and the Fondo Europeo de Desarrollo Regional (FEDER) aimed at the Challenges of Society (Grant No. ENE 2017-83860-R “Nuevos servicios de red para micredes renovables inteligentes. Contribución a la generación distribuida residencial”).

Acknowledgments: The authors would like to thank the University of Jaén for the programmes: “Plan de Apoyo a la I+D+I 2014-2015. Prorrogado hasta 2016 and “Acción 2 «Segunda Fase» comprendida en la “Línea de Actuación: Fomento y divulgación de la transferencia”, enmarcada en el Objetivo 1: “Apoyo a las actividades de transferencia del conocimiento”, del Plan de Apoyo a la Transferencia del Conocimiento, el Emprendimiento y la Empleabilidad año 2017, para la contratación de doctorandos industriales”.

Conflicts of Interest: The authors declare no conflict of interest.

References

1. DNV GL. *Energy Transition Outlook 2018 Oil and Gas*; DNV GL: Oslo, Norway, 2018.
2. Sampaio, P.; González, M. Photovoltaic solar energy: Conceptual framework. *Renew. Sustain. Energy Rev.* **2017**, *74*, 590–601. [[CrossRef](#)]
3. Wang, L.; Wang, Y.; Chen, J. Assessment of the ecological niche of photovoltaic agriculture in China. *Sustainability* **2019**, *11*, 2268. [[CrossRef](#)]
4. Chen, J.; Liu, Y.; Wang, L. Research on coupling coordination development for photovoltaic agriculture system in China. *Sustainability* **2019**, *11*, 1065. [[CrossRef](#)]

5. Bey, M.; Hamidat, A.; Benyoucef, B.; Nacer, T. Viability study of the use of grid connected photovoltaic system in agriculture: Case of Algerian dairy farms. *Renew. Sustain. Energy Rev.* **2016**, *63*, 333–345. [[CrossRef](#)]
6. Gómez-Lorente, D.; Rabaza, O.; Aznar-Dols, F.; Mercado-Vargas, M.J. Economic and environmental study of wineries powered by grid-connected photovoltaic systems in Spain. *Energies* **2017**, *10*, 222. [[CrossRef](#)]
7. Moustafa, K. Toward Future Photovoltaic-Based Agriculture in Sea. *Trends Biotechnol.* **2016**, *34*, 257–259. [[CrossRef](#)]
8. Rabaza, O.; Contreras-Montes, J.; García-Ruiz, M.J.; Delgado-Ramos, F.; Gómez-Lorente, D. Techno-economic performance evaluation for olive mills powered by grid-connected photovoltaic systems. *Energies* **2015**, *8*, 11939–11954. [[CrossRef](#)]
9. Aceite de Oliva. Available online: <https://www.mapa.gob.es/es/agricultura/temas/producciones-agricolas/aceite-oliva-y-aceituna-mesa/aceite.aspx> (accessed on 18 December 2019).
10. Vilar Hernández, J. *Presente y Futuro del Mercado Internacional del Aceite de Oliva*; AES: Malaga, España, 2017.
11. AICA: Agencia de Información y Control Alimentarios. Available online: <http://www.aica.gob.es/> (accessed on 18 December 2019).
12. FAECA. *Manual de Ahorro y Eficiencia Energética del Sector*; FAECA: Madrid, España, 2015.
13. Singh, H.; Sirisamphanwong, C.; Santhi Rekha, S.M. Effect of Tilt and Azimuth Angle on the Performance of PV Rooftop System. *Appl. Mech. Mater.* **2016**, *839*, 159–164. [[CrossRef](#)]
14. Dhimish, M.; Silvestre, S. Estimating the impact of azimuth-angle variations on photovoltaic annual energy production. *Clean Energy* **2019**, *3*, 47–58. [[CrossRef](#)]
15. Mehleri, E.D.; Zervas, P.L.; Sarimveis, H.; Palyvos, J.A.; Markatos, N.C. Determination of the optimal tilt angle and orientation for solar photovoltaic arrays. *Renew. Energy* **2010**, *35*, 2468–2475. [[CrossRef](#)]
16. Kaldellis, J.; Kavadias, K.; Zafirakis, D. Experimental validation of the optimum photovoltaic panels' tilt angle for remote consumers. *Renew. Energy* **2012**, *46*, 179–191. [[CrossRef](#)]
17. Yadav, A.K.; Chandel, S.S. Tilt angle optimization to maximize incident solar radiation: A review. *Renew. Sustain. Energy Rev.* **2013**, *23*, 503–513. [[CrossRef](#)]
18. Morcos, V.H. Optimum tilt angle and orientation for solar collectors in Assiut, Egypt. *Renew. Energy* **1994**, *4*, 291–298. [[CrossRef](#)]
19. Jafarkazemi, F.; Saadabadi, S.A. Optimum tilt angle and orientation of solar surfaces in Abu Dhabi, UAE. *Renew. Energy* **2013**, *56*, 44–49. [[CrossRef](#)]
20. Yakup, M.A.B.H.M.; Malik, A.Q. Optimum tilt angle and orientation for solar collector in Brunei Darussalam. *Renew. Energy* **2001**, *24*, 223–234. [[CrossRef](#)]
21. Kacira, M.; Simsek, M.; Babur, Y.; Demirkol, S. Determining optimum tilt angles and orientations of photovoltaic panels in Sanliurfa, Turkey. *Renew. Energy* **2004**, *29*, 1265–1275. [[CrossRef](#)]
22. Hussein, H.M.S.; Ahmad, G.E.; El-Ghetany, H.H. Performance evaluation of photovoltaic modules at different tilt angles and orientations. *Energy Convers. Manag.* **2004**, *45*, 2441–2452. [[CrossRef](#)]
23. Yang, H.; Lu, L. The optimum tilt angles and orientations of PV claddings for Building-Integrated Photovoltaic (BIPV) applications. *J. Sol. Energy Eng. Trans. ASME* **2007**, *129*, 253–255. [[CrossRef](#)]
24. Paciello, L.; Pedale, A.; Scaradozzi, D.; Conte, G. A design tool for modelling and sizing of energy production/storage home system. In Proceedings of the EESMS 2014—2014 IEEE Workshop on Environmental, Energy and Structural Monitoring Systems Proceedings, Naples, Italy, 17–18 September 2014; pp. 126–131.
25. Vieira, F.M.; Moura, P.S.; de Almeida, A.T. Energy storage system for self-consumption of photovoltaic energy in residential zero energy buildings. *Renew. Energy* **2017**, *103*, 308–320. [[CrossRef](#)]
26. Wolisz, H.; Schütz, T.; Blanke, T.; Hagenkamp, M.; Kohn, M.; Wesseling, M.; Müller, D. Cost optimal sizing of smart buildings' energy system components considering changing end-consumer electricity markets. *Energy* **2017**, *137*, 715–728. [[CrossRef](#)]
27. Şenol, M.; Abbasoğlu, S.; Kükrer, O.; Babatunde, A.A. A guide in installing large-scale PV power plant for self consumption mechanism. *Sol. Energy* **2016**, *132*, 518–537. [[CrossRef](#)]
28. Luthander, R.; Widén, J.; Nilsson, D.; Palm, J. Photovoltaic self-consumption in buildings: A review. *Appl. Energy* **2015**, *142*, 80–94. [[CrossRef](#)]
29. Salvador, M.; Grieu, S. Methodology for the design of energy production and storage systems in buildings: Minimization of the energy impact on the electricity grid. *Energy Build.* **2012**, *47*, 659–673. [[CrossRef](#)]

30. Castillo-Cagigal, M.; Caamaño-Martín, E.; Matallanas, E.; Masa-Bote, D.; Gutiérrez, A.; Monasterio-Huelin, F.; Jiménez-Leube, J. PV self-consumption optimization with storage and Active DSM for the residential sector. *Sol. Energy* **2011**, *85*, 2338–2348. [CrossRef]
31. Al Garni, H.; Awasthi, A. Techno-Economic Feasibility Analysis of a Solar PV Grid-Connected System with Different Tracking Using HOMER Software. In Proceedings of the 2017 IEEE International Conference on Smart Energy Grid Engineering (SEGE), Oshawa, ON, Canada, 14–17 August 2017; pp. 217–222.
32. Sinha, S.; Chandel, S.S. Review of software tools for hybrid renewable energy systems. *Renew. Sustain. Energy Rev.* **2014**, *32*, 192–205. [CrossRef]
33. Ghiani, E.; Vertuccio, C.; Pilo, F. Optimal Sizing and Management of a Smart Microgrid for Prevailing Self-Consumption. In Proceedings of the 2015 IEEE Eindhoven PowerTech, Eindhoven, The Netherlands, 29 June–2 July 2015; pp. 1–6.
34. Ghiani, E.; Giordano, A.; Nieddu, A.; Rosetti, L.; Pilo, F. Planning of a Smart Local Energy Community: The Case of Berchidda Municipality (Italy). *Energies* **2019**, *12*, 4629. [CrossRef]
35. Martín-Chivelet, N.; Montero-Gómez, D. Optimizing photovoltaic self-consumption in office buildings. *Energy Build.* **2017**, *150*, 71–80. [CrossRef]
36. Poulek, V.; Dang, M.; Libra, M.; Beránek, V.; Šafránková, J. PV Panel With Integrated Lithium Accumulators For BAPV Applications—One Year Thermal Evaluation. *IEEE J. Photovoltaics* **2020**, *10*, 150–152. [CrossRef]
37. Yu, H.; Duan, J.; Du, W.; Xue, S.; Sun, J. China’s energy storage industry: Develop status, existing problems and countermeasures. *Renew. Sustain. Energy Rev.* **2017**, *71*, 767–784. [CrossRef]
38. Lave, M.; Kleissl, J.; Arias-Castro, E. High-frequency irradiance fluctuations and geographic smoothing. *Sol. Energy* **2012**, *86*, 2190–2199. [CrossRef]
39. Zawilska, E.; Brooks, M.J. An assessment of the solar resource for Durban, South Africa. *Renew. Energy* **2011**, *36*, 3433–3438. [CrossRef]
40. Journée, M.; Müller, R.; Bertrand, C. Solar resource assessment in the Benelux by merging Meteosat-derived climate data and ground measurements. *Sol. Energy* **2012**, *86*, 3561–3574. [CrossRef]
41. Gueymard, C.A.; Wilcox, S.M. Assessment of spatial and temporal variability in the US solar resource from radiometric measurements and predictions from models using ground-based or satellite data. *Sol. Energy* **2011**, *85*, 1068–1084. [CrossRef]
42. Jiménez-Torres, M.; Rus-Casas, C.; Lemus-Zúñiga, L.G.; Hontoria, L. The importance of accurate solar data for designing solar photovoltaic systems—Case studies in Spain. *Sustainability* **2017**, *9*, 247. [CrossRef]
43. Hontoria, L.; Rus-Casas, C.; Aguilar, J.D.; Hernandez, J.C. An improved method for obtaining solar irradiation data at temporal high-resolution. *Sustainability* **2019**, *11*, 5233. [CrossRef]
44. Hirsch, T.; Schenk, H.; Schmidt, N.; Meyer, R. Dynamics of oil-based parabolic trough plants—Impact of transient behaviour on energy yields. In Proceedings of the SolarPACES 2010 Conference, Perpignan, France, 21–24 September 2010.
45. Moreno-Tejera, S.; Silva-Pérez, M.A.; Lillo-Bravo, I.; Ramírez-Santigosa, L. Solar resource assessment in Seville, Spain. Statistical characterisation of solar radiation at different time resolutions. *Sol. Energy* **2016**, *132*, 430–441. [CrossRef]
46. Sandia National Laboratories. *Stand-Alone Photovoltaic Systems: A Handbook of Recommended Design Practices*; Absorpt. Fluids Data Surv. Final Rep. Foreign Data; Sandia National Laboratories: Albuquerque, NM, USA, 1995; pp. 1–437.
47. Carroquino, J.; Dufo-López, R.; Bernal-Agustín, J.L. Sizing of off-grid renewable energy systems for drip irrigation in Mediterranean crops. *Renew. Energy* **2015**, *76*, 566–574. [CrossRef]
48. Radiación Solar. Available online: <https://www.agenciaandaluzadelaenergia.es/Radiacion/radiacion1.php> (accessed on 20 October 2019).
49. Rus-Casas, C.; Aguilar, J.D.; Rodrigo, P.; Almonacid, F.; Pérez-Higueras, P.J. Classification of methods for annual energy harvesting calculations of photovoltaic generators. *Energy Convers. Manag.* **2014**, *78*, 527–536. [CrossRef]
50. IEC. *IEC 61724-1 Edition 1.0 2017-03 Photovoltaic System Performance—Part 1: Monitoring IEC*, 1st ed.; IEC Publications: Geneva, Switzerland, 2017; ISBN 9782832239889.
51. Jiménez-Castillo, G.; Muñoz-Rodríguez, F.J.; Rus-Casas, C.; Talavera, D.L. A new approach based on economic profitability to sizing the photovoltaic generator in self-consumption systems without storage. *Renew. Energy* **2020**, *148*, 1017–1033. [CrossRef]

52. Talavera, D.L.; Muñoz-Rodríguez, F.J.; Jimenez-Castillo, G.; Rus-Casas, C. A new approach to sizing the photovoltaic generator in self-consumption systems based on cost-competitiveness, maximizing direct self-consumption. *Renew. Energy* **2019**, *130*, 1021–1035. [[CrossRef](#)]
53. Mubarak, R.; Luiz, E.W.; Seckmeyer, G. Why PV Modules Should Preferably No Longer Be Oriented to the South in the Near Future. *Energies* **2019**, *12*, 4528. [[CrossRef](#)]
54. Burgio, A.; Menniti, D.; Sorrentino, N.; Pinnarelli, A.; Leonowicz, Z. Influence and impact of data averaging and temporal resolution on the assessment of energetic, economic and technical issues of hybrid photovoltaic-battery systems. *Energies* **2020**, *13*, 354. [[CrossRef](#)]
55. Guerra, T.A.; Guerra, J.A.; Tabernero, B.O.; De La Cruz García, G. Comparative energy performance analysis of six primary photovoltaic technologies in Madrid (Spain). *Energies* **2017**, *10*, 772. [[CrossRef](#)]
56. Mondol, J.D.; Yohanis, Y.G.; Smyth, M.; Norton, B. Performance analysis of a grid-connected building integrated photovoltaic system. In Proceedings of the ISES 2003: ISES Solar World Congress 2003: Solar Energy for a Sustainable Future, Göteborg, Sweden, 14–19 June 2003.
57. Šúri, M.; Huld, T.A.; Dunlop, E.D.; Ossenbrink, H.A. Potential of solar electricity generation in the European Union member states and candidate countries. *Sol. Energy* **2007**, *81*, 1295–1305. [[CrossRef](#)]
58. Ransome, S.J.; Wohlgemuth, J.H. kWh/kWp dependency on PV technology and balance of systems performance. In Proceedings of the Conference Record of the Twenty-Ninth IEEE Photovoltaic Specialists Conference, New Orleans, LA, USA, 19–24 May 2002; pp. 1420–1423.
59. Ruiz-Arias, J.A.; Terrados, J.; Pérez-Higueras, P.; Pozo-Vázquez, D.; Almonacid, G. Assessment of the renewable energies potential for intensive electricity production in the province of Jaén, southern Spain. *Renew. Sustain. Energy Rev.* **2012**, *16*, 2994–3001. [[CrossRef](#)]
60. Almonacid, F.; Rus, C.; Hontoria, L.; Muñoz, F.J.; Fuentes, M.; Nofuentes, G. Characterisation of Si-crystalline PV modules by artificial neural networks. *Renew. Energy* **2009**, *34*, 941–949. [[CrossRef](#)]
61. Almonacid, F.; Rus, C.; Pérez, P.J.; Hontoria, L. Estimation of the energy of a PV generator using artificial neural network. *Renew. Energy* **2009**, *34*, 2743–2750. [[CrossRef](#)]
62. Tina, G.M.; Ventura, C.; Sera, D.; Spataru, S. Comparative Assessment of PV Plant Performance Models Considering Climate Effects. *Electr. Power Components Syst.* **2017**, *45*, 1381–1392. [[CrossRef](#)]
63. Poulek, V.; Matuška, T.; Libra, M.; Kachalouski, E.; Sedláček, J. Influence of increased temperature on energy production of roof integrated PV panels. *Energy Build.* **2018**, *166*, 418–425. [[CrossRef](#)]
64. Jiménez-Castillo, G.; Tina, G.-M.; Muñoz-Rodríguez, F.-J.; Rus-Casas, C. Smart meters for the evaluation of self-consumption in zero energy buildings. In Proceedings of the 2019 10th International Renewable Energy Congress (IREC), Sousse, Tunisia, 26–28 March 2019; pp. 1–6.
65. Iqbal, M. *An Introduction to Solar Radiation*; Elsevier: Amsterdam, The Netherlands, 2012; ISBN 0323151817.
66. Cao, S.; Sirén, K. Impact of simulation time-resolution on the matching of PV production and household electric demand. *Appl. Energy* **2014**, *128*, 192–208. [[CrossRef](#)]
67. Ayala-Gilardón, A.; Sidrach-de-Cardona, M.; Mora-López, L. Influence of time resolution in the estimation of self-consumption and self-sufficiency of photovoltaic facilities. *Appl. Energy* **2018**, *229*, 990–997. [[CrossRef](#)]
68. Wolf, P.; Včelák, J. Simulation of a simple PV system for local energy usage considering the time resolution of input data. *J. Energy Storage* **2018**, *15*, 1–7. [[CrossRef](#)]
69. Wyrsh, N.; Riesen, Y.; Ballif, C. Effect of the fluctuations of pv production and electricity demand on the pv electricity self-consumption. In Proceedings of the 28th European Photovoltaic Solar Energy Conference and Exhibition, Villepinte, France, 30 September–4 October 2013; pp. 4322–4324.
70. Jiménez-Castillo, G.; Muñoz-Rodríguez, F.J.; Rus-Casas, C.; Gómez-Vidal, P. Improvements in Performance Analysis of Photovoltaic Systems: Array Power Monitoring in Pulse Width Modulation Charge Controllers. *Sensors* **2019**, *19*, 2150. [[CrossRef](#)] [[PubMed](#)]
71. Muñoz, F.J.; Jiménez, G.; Fuentes, M.; Aguilar, J.D.; Munoz, F.J.; Jimenez-Castillo, G.; Fuentes, M.; Aguilar, J.D. Power Gain and Daily Improvement Factor in Stand-Alone Photovoltaic Systems With Maximum Power Point Tracking Charge Regulators. Case of Study: South of Spain. *J. Sol. Energy Eng. ASME* **2013**, *135*, 1–9. [[CrossRef](#)]
72. Rus-Casas, C.; Hontoria, L.; Fernández-Carrasco, J.; Jiménez-Castillo, G.; Muñoz-Rodríguez, F.J. Development of a Utility Model for the Measurement of Global Radiation in Photovoltaic Applications in the Internet of Things (IoT). *Electronics* **2019**, *8*, 304.

73. Jiménez-Castillo, G.; Muñoz-Rodríguez, F.; Rus-Casas, C.; Hernández, J.C.; Tina, G. Monitoring PWM signals in stand-alone photovoltaic systems. *Measurement* **2019**, *134*, 412–425.
74. Widén, J.; Wäckelgård, E.; Paatero, J.; Lund, P. Impacts of different data averaging times on statistical analysis of distributed domestic photovoltaic systems. *Sol. Energy* **2010**, *84*, 492–500. [[CrossRef](#)]
75. Sørnes, K.; Fredriksen, E.; Tunheim, K.; Sartori, I. Analysis of the impact resolution has on load matching in the Norwegian context. *Energy Procedia* **2017**, *132*, 610–615. [[CrossRef](#)]
76. Beck, T.; Kondziella, H.; Huard, G.; Bruckner, T. Assessing the influence of the temporal resolution of electrical load and PV generation profiles on self-consumption and sizing of PV-battery systems. *Appl. Energy* **2016**, *173*, 331–342. [[CrossRef](#)]
77. Shukla, A.K.; Sudhakar, K.; Baredar, P. A comprehensive review on design of building integrated photovoltaic system. *Energy Build.* **2016**, *128*, 99–110. [[CrossRef](#)]



© 2020 by the authors. Licensee MDPI, Basel, Switzerland. This article is an open access article distributed under the terms and conditions of the Creative Commons Attribution (CC BY) license (<http://creativecommons.org/licenses/by/4.0/>).